The Polyhedral State of Molecular Matter

Arnout Ceulemans*[a] and Erwin Lijnen[a]

Keywords: Group theory / Topological chemistry / Polyhedra / Fullerenes / Cubanes / Boranes

The review introduces the mathematical concept of a complex, as an original way to describe the topology of a polyhedral molecule. It shows how this concept can be applied to electronic structures and magnetic and vibrational properties. Using symmetry it identifies topologically invariant orbitals and moments.

1. Introduction

A molecule is a set of atomic nuclei held together by a cloud of electrons. In its simplest representation this form of matter can be conceived as a collection of beads held together by strings. The mathematical concept, which corresponds to this representation, is the concept of a *graph*.[1] In the graph-like state only the connections between atoms count, and there is no information on their spatial arrangement. Nonetheless this representation is extremely useful, not only to retrieve molecules in a data-base, but also to rationalise many important molecular properties.[2]

The topic of this review will be a higher form of molecular organisation, which we describe as the *polyhedral* state. Inorganic chemists already have an intuitive knowledge of polyhedra, as structural units of many inorganic compounds. In its polyhedral state, molecular matter is not just a set of points and lines, but it is furthermore specified that certain closed loops of lines will form faces. In turn faces themselves may enclose a finite region of space which is a cell or a chamber. The mathematical concept, which corresponds to this polyhedral representation, is the concept of a *polyhedral complex*.[3]

Unlike its graph relative, the complex concept is not known outside mathematics. In section 2 we will thus first have to explain its proper meaning. For this no special mathematical background will be required, except for a general knowledge of group theory for chemists, as may be found in Cotton's book.[4] In section 3 we will then represent a fundamental result about the symmetries of polyhedral complexes, which opens up this concept for applications on molecular matter. In the subsequent sections, several applications related to electronic structure and elastic and magnetic properties of network molecules are reviewed.

2. Polyhedral Complexes

In the chemical literature a polyhedron refers to a surface which is wrapped around a finite region of space, and consists of many polygons or faces; in turn the faces are bor-

[a] Division of Quantum Chemistry, Katholieke Universiteit Leuven,
Celestijnenlaan 200F, 3001 Leuven, Belgium
Fax: (internat.) + 32-16/327992
E-mail: Arnout.Ceulemans@chem.kuleuven.ac.be

Arnout Ceulemans (left) is full Professor of Chemistry at the University of Leuven. He received his Ph. D. in Leuven while working in the group of Luc Vanquickenborne on theoretical models for ligand field photochemistry. He habilitated in 1986 in Leuven with a thesis on the Jahn−Teller effect in complexes and clusters. He teaches Group Theory, Chemical Physics, and Inorganic Chemistry. His main research interests are the application of group-theoretical and topological methods at the border between chemistry and physics.

Erwin Lijnen (right) graduated in chemistry at the University of Leuven in 2001. He is currently Aspirant of the Fund for Scientific Research − Flanders (Belgium) and prepares a doctoral thesis in the laboratory of Quantum Chemistry at the K. U. Leuven on topological representations of tridimensional molecular structures.

MICROREVIEWS: This feature introduces the readers to the authors' research through a concise overview of the selected topic. Reference to important work from others in the field is included.

dered by edges; finally the edges connect vertices. Chemists are also familiar with Euler's celebrated theorem that states that the numbers of vertices, edges, and faces, denoted as v, e, and f, respectively, obey the rule as given in Equation (1).

$$v - e + f = 2 \tag{1}$$

This theorem holds for any polyhedron that can be mapped on the surface of a sphere.[5] It can, however, be generalised to polyhedral nets on surfaces with other topologies as shown in Equation (2).

$$v - e + f = \chi \tag{2}$$

Here χ is a fixed integer, the Euler characteristic, which marks the particular topology of the surface on which the polyhedron is embedded. As an example for a sphere with g handles or holes, the Euler characteristic reads as given in Equation (3) with $g = 0$ for a sphere, $g = 1$ for a torus or doughnut, $g = 2$ for a pretzel etc.; g is also called the genus of the surface.

$$\chi = 2 - 2g \tag{3}$$

Turning from chemistry to mathematics we must now become acquainted with the ingredients of the polyhedral complex in the mathematical sense. Of course the same structural elements, vertices, edges, and faces, will appear, but there are some nontrivial amendments, and, above all, we must find out what happens to the Euler characteristic.

Vertices are zero-dimensional objects, and therefore are trivial. A given vertex will be denoted as v^i. At the next level, an edge is already not just a line connecting two vertices, but rather an arrow, pointing from one of these vertices to the other. Hence an edge between two vertices, say v^i and v^j will be denoted as the *ordered* pair $(v^i v^j)$, where we agree to identify the first vertex, v^i, as the tail of the arrow, and the second, v^j, as its head. The ordering itself is purely a matter of choice. We might as well denote the same edge by the inverted ordering, $(v^j v^i)$. Since the corresponding arrow points in the opposite direction, we can write Equation (4).

$$(v^i v^j) = -(v^j v^i) \tag{4}$$

The requirement that the edges be ordered is therefore not just a trivial feature: it transforms the edges to signed quantities, and therefore creates algebra on the surface of the polyhedron. At this point it is of course difficult to appreciate all its implications, but we hope this will gradually become clear in the forthcoming sections.

In a similar way a face is an ordered closed loop of vertices. Consider for instance three vertices, say v^i, v^j, and v^k, which form a triangular face, then we may denote this face as the ordered trio $(v^i v^j v^k)$. This notation defines the face as a closed loop, $v^i \rightarrow v^j \rightarrow v^k \rightarrow v^i$. For an external observer this circulation will have a definite sense, either clockwise or anticlockwise. Again if we invert the ordering, we invert this sense, and we can write Equation (5).

$$(v^i v^j v^k) = -(v^k v^j v^i) \tag{5}$$

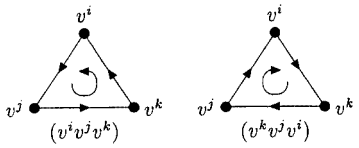

Vertices, edges, and faces are layers of organisation, involving objects of dimension zero (point), one (line), and two (plane), respectively. We could also include the next layer of 3D objects or cells, but will not further consider this here.

As in all organised structures consecutive layers are in touch. The topdown descent from higher to lower dimensional objects is called *bordering* or *taking the boundary.*

The boundary of a face is a sum of the arrows along the surrounding edges. We will avoid the rigorous mathematical definition of this operation and write it in a simple pictorial way as

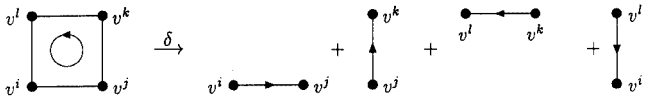

or as

$$\delta(v^i\ v^j\ v^k\ v^l) = (v^i\ v^j) + (v^j\ v^k) + (v^k\ v^l) + (v^l\ v^i)$$

where the Greek letter δ represents the boundary operation. Likewise the boundary of an edge is the difference between its head vertex and its tail

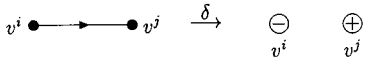

or

$$\delta(v^i\ v^j) = v^j - v^i.$$

Interestingly, not all combinations of a given level have boundaries. As an example, when the number of incoming and outgoing arrows on a given vertex is the same, this vertex is not a boundary, e.g.

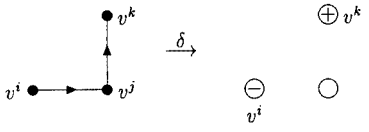

This part of the theory is the most interesting from our point of view: we must look for combinations that are not boundaries of some higher level, and have no boundaries on some lower level. Such combinations are *topological invariants* of the polyhedron, and are extremely important from the point of view of electronic structures. In mathematics they are called *homologies*.[6] These are the concepts behind the Euler characteristic. Our task will be to identify them properly, since they hold the key to the topology. To summarise, in Table 1 we list the ingredients of a tetrahedral complex. This complex can be embedded on a sphere and therefore has Euler characteristic $\chi = 2$. It indeed contains two homologies, which we will try to find in the next section with the help of group theory.

Table 1. Elements of a tetrahedral complex

Vertices or Atoms	Edges or Bonds	Faces
v^0	(v^0v^1)	$(v^0v^1v^2)$
v^1	(v^0v^2)	$(v^0v^1v^3)$
v^2	(v^0v^3)	$(v^0v^2v^3)$
v^3	(v^1v^2)	$(v^1v^2v^3)$
	(v^1v^3)	
	(v^2v^3)	

3. From Topology to Symmetry and Back

If the polyhedron exhibits a point-group symmetry, we can apply its symmetry elements to the set of vertices. The action of a symmetry element on a vertex is very simple: it just maps this vertex on some other vertex of the complex. It therefore can be described as a permutation of the elements in the set of vertices. Hence we can write Equation (6), where R_i is the image of i under this mapping.

$$Rv^i = v^{R_i} \tag{6}$$

This expression is all one needs to determine how the ordered objects, edges and faces, of the polyhedral complex behave under symmetry operations. Indeed one has for an ordered pair Equation (7).

$$R(v^iv^j) = (v^{R_i}v^{R_j}) \tag{7}$$

The resulting image $(v^{Ri}v^{Rj})$ is again an edge, which will also belong to the complex, although it might have been defined in opposite order as $(v^{Rj}v^{Ri})$ in which case we can always rewrite the equation as Equation (8).

$$R(v^iv^j) = -(v^{R_j}v^{R_i}) \tag{8}$$

Similarly, mapping of face circulations under symmetry elements may produce images that differ by a sign from the selected list of faces, but in any case a face will always be mapped by R on another face which will be symmetric to the former one.

In this way we can easily determine the transformation matrices describing the action of the symmetry elements on the components of the polyhedral complex. These matrices form representations of the symmetry group. In Table 2 we introduce appropriate symbols for the representations of vertices, edges and faces.

Table 2. Symmetry representation for the elements of a complex

Element	Symbol	Type
vertex	$\Gamma_\sigma(v)$	scalar
edge	$\Gamma_\parallel(e)$	vector
face	$\Gamma_\odot(f)$	rotor

Here Γ is the general symbol for induced symmetry representations.[7] The index σ for the vertex representations indicates that point vertices are symmetric objects with respect to the symmetry elements that pass through the vertex sites, in the same way as s or p_z orbitals in axially symmetric sites. For the edge representations the symbol $\parallel$ refers to the set of arrows along the edges, while the index $\odot$ in the face-representations refers to the circular arrows on the faces. All these representations are in principle *reducible*, which means that they can be decomposed into standard irreducible representations, which describe the basic symmetry patterns in the point group.

These so-called *irreps* can easily be found using the standard techniques of character theory.[4] As an example for the tetrahedral complex in Table 1, one immediately obtains these representations in the T_d symmetry group, see Equation (9).

$$\begin{aligned} \Gamma_\sigma(v) &= A_1 + T_2 \\ \Gamma_\parallel(e) &= T_1 + T_2 \\ \Gamma_\odot(f) &= A_2 + T_1 \end{aligned} \tag{9}$$

Of these combinations only the vertex terms are familiar to chemists. They simply represent the SALCs (symmetry-adapted linear combinations of atomic orbitals) of MO (molecular orbitals) theory, and look as follows.

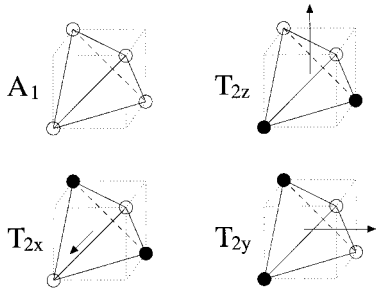

The representations on the edges can be constructed in an entirely similar way, only the constituent objects are not s-like orbitals on the atomic vertices, but with arrows along the edges. As an example we show the z components of T_1 and T_2. In the T_{2z} combination the tetrahedron is oriented in the upright z direction, and the arrows along the four lateral edges are pointing upwards. The same arrows are present in the T_{1z} combination but now their orientation alternates between pointing up and down. The x and y components are oriented in an analogous way along their respective directions.

Finally the face terms correspond to symmetry-adapted linear combinations of circular arrows on the face centres. Here we show the A_2 and T_{1z} components.

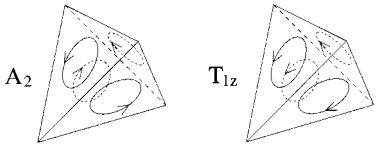

In Figure 1 we gather all these components in a schematic overview. We have also added the boundary relations that exist between the different layers, to this figure. It is very important to realise that taking the boundaries of faces or edges will *not* alter the symmetries. This operation indeed simply corresponds to the expansion of the circular face arrows to the bordering edges and the edge arrows to the head and tail vertices. As a result, the T_1 face terms will be bordered by the equisymmetric T_1 edge terms, while the T_2 edge modes indeed are bordered by the equisymmetric T_2 vertex combinations.

Two combinations stand on their own, not being bordered by a lower ranking component, nor being themselves borders of some higher component: the A_1 vertex combination and the A_2 face combination. Indeed by taking the boundary of the latter, we generate on all edges pairs of opposite arrows, which therefore cancel. Similarly, the former cannot be the boundary of an edge mode, since all vertices have the same weight, implying no net changes along edges.

Hence by using symmetry and elimination we have found combinations, which are very special topological invariants: they cannot be the origin or image of the boundary mapping.

These combinations can easily be filtered out by taking the alternating sum of all three representations, Equation (10).

$$\Gamma_\sigma(v) - \Gamma_\parallel(e) + \Gamma_\odot(f) = A_1 + T_2 - T_1 - T_2 + A_2 + T_1 = A_1 + A_2 \tag{10}$$

Indeed in this way all terms which are taking part in the boundary will cancel.

Obviously, the structure of Equation (10) involves the familiar Euler theorem for a surface of genus zero. Indeed if we ignore all symmetry elements, or equivalently suppose that the only symmetry element is the trivial unit element of the point group, all representations in Equation (10) would reduce to multiples of the trivial A representation of the C_1 point group, and the multiplication factor would simply

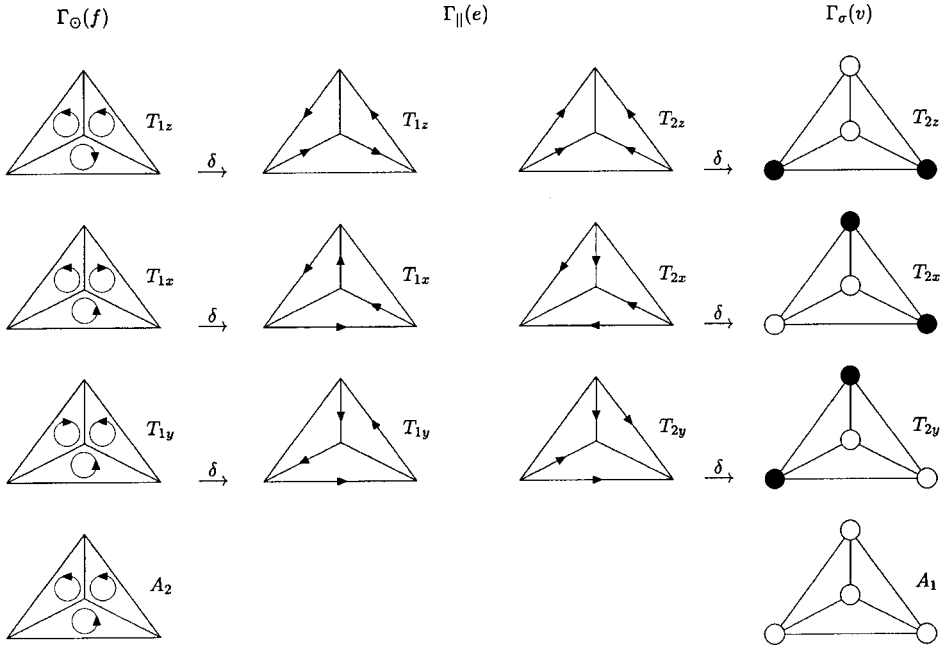

Figure 1. SALCs for the tetrahedral complex

equal the number of vertices, edges, or faces, see Equation (11).

$$\begin{aligned} \Gamma_\sigma(v) &= v.A \\ \Gamma_\parallel(e) &= e.A \\ \Gamma_\odot(f) &= f.A \end{aligned} \tag{11}$$

With $A_1 + A_2 \rightarrow 2\ A$, Equation (10) then reduces to a purely dimensional formula, $v - e + f = 2$, which is exactly Euler's result. Hence, by bringing together symmetry and topology, it is possible to reveal the topological aspects of Euler's rule:

1. We understand now that, not only are the numbers of the polyhedral structure elements related, but also their symmetries. In this respect the number rule is just the (dimensional) top of a symmetry iceberg.

2. The topological invariants, which appear as the remainders of the alternating sum over the structural layers, are characterised by irreducible symmetry representations. These symmetries are keys to relating the topological invariants to chemical and physical properties.

For polyhedra, which can be mapped on the surface of a sphere, the result in Equation (10) can be cast in the general form as given in Equation (12).

$$\Gamma_\sigma(v) - \Gamma_\parallel(e) + \Gamma_\odot(f) = \Gamma_0 + \Gamma_\epsilon \tag{12}$$

The representations Γ_0 and Γ_ε, which appear here on the right-hand side are, respectively, the totally symmetric and pseudo-scalar representation, which is symmetric under proper rotations and antisymmetric under improper rotations. In Mulliken's notation for the point groups, the Γ_0 representation receives labels such as: A_1, A_{1g}, or $A_1{}'$, while the corresponding Γ_ε representation is denoted as A_2, A_{2u}, or $A_2{}''$. A general proof of this result has been given,[8] and its connection to the abstract theory of homology groups has been explained.[9]

Similar results can be obtained for polyhedra with other Euler characteristics. In each case the alternating sum of representations will generate a characteristic set of homologies.

In Table 3 we give an overview of the different topologies we have examined so far. The final two items in the table concern polyhedra that are embedded on a 3D surface. In this case a further structural element must be added, which is the cell or chamber. In the same way as faces are defined as rings of edges, cells are closed regions of space surrounded by faces. In this case the Euler theorem must be extended to include the number of cells, c: Equation (13).

$$v - e + f - c = \chi \tag{13}$$

As an example in the case of a body-centred tetrahedron one has $v = 5$, $e = 10$, $f = 10$, $c = 4$, resulting in the Euler characteristic $\chi = 1$, as indicated in Table 3 for polyhedra with the topology of a solid sphere.

Table 3. Overview of topological structures for which symmetry relationships have been derived

Topology	χ	Polyhedron	Example	Ref.
hollow sphere (2D)	2	deltahedron	*closo*-boranes	[8]
		trivalent	fullerenes	[8]
torus (2D)	0	deltahedron	-	[11]
		trivalent	carbon toroid	[11]
double torus (2D)	-2	pretzel	-	[11]
		triple hoop	-	[11]
disk (2D)	1	polyhex	benzenoid	[11]
plane (2D)	0	2D periodic lattice	graphite sheet	[12]
negative curvature surfaces (2D)	-4	trivalent	schwarzites	[13]
solid sphere (3D)	1	centred	-	-
		concentric	multishell clusters	[10]
space (3D)	0	3D periodic lattice	diamond	[12]

4. Applications

In this section we review two typical cases of polyhedral electronic structures and identify the topologically determined properties.

4.1 The Antibonding Orbitals in Trivalent Clusters

Electron counting rules are an important tool for addressing the problem of cluster bonding, and new developments continue to appear.[14,15] Here we will examine a straightforward application of the general graph-theoretical result, which is encountered in the electronic structure of so called "electron-precise" trivalent clusters.[8]

In a trivalent polyhedral cage, each cluster atom has three neighbours. From each vertex radiate three edges, while in turn every edge is linked to two vertices, see Equation (14).

$$3v = 2e \tag{14}$$

The cluster will be completely edge-bonding if each cluster atom has three valence orbital hybrids, which point along the edges and are each occupied by one electron. This requires one inward pointing (radial) hybrid and a tangential $\{p_x, p_y\}$ pair.

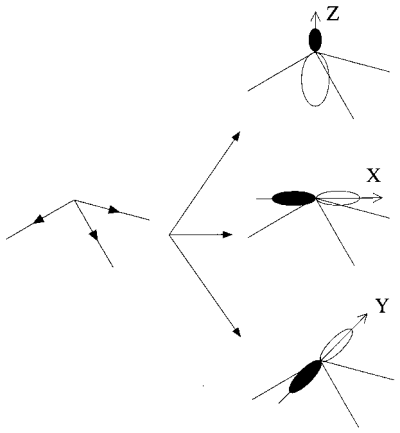

In this way one obtains a saturated or "electron-precise" electronic structure with precisely $3v/2$ valence electron pairs, forming an equal number of σ bonds along the edges. Examples are the polyhedranes C_vH_v such as tetrahedrane ($v = 4$), cubane ($v = 8$), or dodecahedrane ($v = 20$), or the equivalent transition-metal clusters, built on the isolobal $Co(CO)_3$ or $Ir(CO)_3$ fragments.[16]

The electronic levels of such compounds were investigated by Johnston and Mingos.[17,18] The $3v/2$ occupied bonding orbitals have precisely $3v/2$ antibonding counterparts. These empty orbitals on the edges can be grouped together in $[v/2] + 1$ strongly antibonding face-combinations and $v - 1$ less antibonding vertex-localised orbitals, Equation (15).

$$3v/2 = [v/2 + 1] + [v - 1] \tag{15}$$

Since in a trivalent cage one has $3v = 2e$ [Equation (14)] and $f = v/2 + 2$, Equation (15) is just a manifestation of Euler's rule, written as in Equation (16).

$$e = [f - 1] + [v - 1] \tag{16}$$

We can now extend this rule to the symmetries of these antibonds. Antibonds along edges with a positive head and a negative tail have precisely the same symmetry as arrows along edges, hence the symmetries of the antibonding shell correspond to $\Gamma_{\|}(e)$.

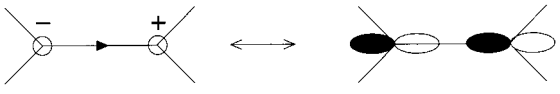

The symmetry result then predicts Equation (17).

$$\begin{array}{rcccc} e & = & [f-1] & + & [v-1] \\ \Gamma_{\|}(e) & = & [\Gamma_{\odot}(f) - \Gamma_{\epsilon}] & + & [\Gamma_{\sigma}(v) - \Gamma_0] \end{array} \tag{17}$$

The first term on the right-hand side of dimension $(f - 1)$ refers to symmetries of faces in the polyhedral complex. We have represented these earlier as circular arrows, which indeed precisely correspond to the face antibonds of Mingos and Johnston.

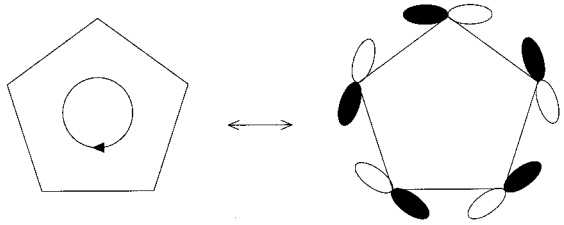

The topological basis of this result clearly explains why the number of these highly antibonding orbitals is one less than the number of faces. Indeed if we set up an antibonding combination in which all the face antibonds are rotating in the same direction, there will be two opposite arrows along every edge, which will therefore exactly cancel.

The second term of the equation contains the remaining $v - 1$ terms, which are vertex-localised and therefore less antibonding, as was found by the previous model calculations of Johnston and Mingos.[17] Again the topology of the polyhedron explains why the number of these is one less than the number of vertices. The combination that is lacking transforms as Γ_0, and simply corresponds to the sum of all vertex orbitals of σ-type. This combination is of course completely bonding, and cannot be contained in the edge-antibonding orbitals.

We thus have found important features of the electronic structure of trivalent clusters, which clearly belong to the polyhedral state of molecular matter. The repartitioning of the edge antibonds in face-related and vertex-related parts is entirely based on the polyhedral relationships, as expressed by the symmetry extension of Euler's rule. In electron-precise compounds both sets are empty, yielding an electron count of $3v/2$ skeletal pairs.

4.2 Electronic Properties of Toroidal Polyhedra

The invariants, which arise in the abstract topological treatment, can be understood very simply in terms of densities and currents on a polyhedral surface.

As a simple physical example we take a model of fluid flow on a polyhedral surface. One could think of a flooded polyhedron, with observers on the vertices, edge centres, and face centres. The observers on the vertices measure the net increase or decrease in density which is taking place at the vertices during a given time interval. They thus report a scalar quantity, which stands for the vertex term in the expression. The observers on the edges measure the fluid flow along the edges. The quantity that they report is a vectorial component of flow pointing along the direction of the edge; this is precisely the edge term in the expression. Finally, the observers on the faces measure net circular currents going around the face centres. This corresponds to a component of a rotor, perpendicular to the face, as is expressed by the face term. The theorem then makes a comparison of these three reports: it finds that the flow along the edges exactly accounts for the net changes of density on

the vertices and net circulation around the face centres, except for two modes, which leave no trace in the bookkeeping of the edge currents: the simultaneous increase of density on all vertices, the Γ_0 term, and the simultaneous rotatory currents on all faces in the same sense, as expressed by the Γ_ε term.

If the fluid consists of electrons, the first term represents changes of the total electrical charge of the polyhedron. This mode will be zero if charge is conserved. It cannot give rise to charge flows over the network.

The second mode is less trivial, but in fact equally fundamental. It represents the total magnetic charge of the polyhedral cluster. Electromagnetism requires this charge to be zero, in the absence of magnetic monopoles. Hence both modes refer to conserved quantities which cannot be generated or annihilated by external fields.

In this respect toroidal polyhedra, i.e. polyhedral networks that can be mapped on the surface of a torus or doughnut, offer far more interesting perspectives, since they have topological invariants that have the symmetry of electric and magnetic dipoles.

For a toroidal polyhedron, the Euler theorem reads as in Equation (18).

$$v - e + f = 0 \tag{18}$$

The zero on the right-hand side hides no less than four topological invariants, which make their appearance when the theorem is written in symmetry form, Equation (19).

$$\Gamma_\sigma(v) - \Gamma_\parallel(e) + \Gamma_\odot(f) = \Gamma_0 + \Gamma_\epsilon - \Gamma(T_z) - \Gamma(R_z) \tag{19}$$

The two negative terms on the right-hand side that were absent in the globular polyhedra, are the irreducible symmetry representations of the translation along the central symmetry axis of the torus (T_z), and of the rotation about the same axis (R_z). Both these terms refer to special combinations of edge arrows which have no boundaries at the vertices, and do not interfere with face circulations.[11] These modes are represented by circular motions going around the torus as shown in Figure 2. The $\Gamma(T_z)$ mode corresponds to a circulation linking the inside and outside of the toroidal ring. It is antisymmetric with respect to the inversion centre and horizontal symmetry plane, and symmetric under the principal rotational symmetry axis, exactly as a translation mode in the z direction. On the other hand the $\Gamma(R_z)$ mode constitutes a circulation about the principal axis. It is also symmetrical under this axis, as well as under the inversion centre and the horizontal symmetry plane.

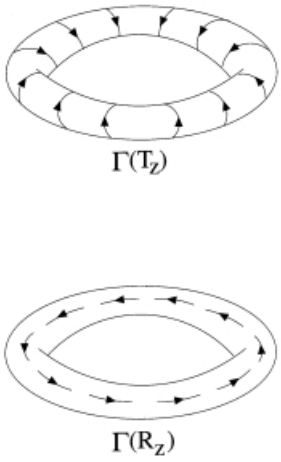

Figure 2. Topologically invariant edge currents on a torus, transforming as translation $\Gamma(T_z)$ and rotation $\Gamma(R_z)$

In ideal cylindrical symmetry, $D_{\infty h}$, these terms match the symmetry representations Σ_u^+ and Σ_g^- which are, respectively, the symmetries of the electric and magnetic dipole. Interestingly, both these invariants can be introduced by external fields. If one places a toroidal polyhedron in a homogeneous magnetic field, with its z axis parallel to the direction of the field, one will indeed induce circular bond currents on the torus, which correspond to the $\Gamma(R_z)$ mode. Open-shell molecules can furthermore sustain spontaneous currents that have precisely this topology.

In contrast, the second mode, $\Gamma(T_z)$, is much subtler. It introduces a moment that is known from nuclear physics[19] as an "anapole" moment. If one simply places the torus in a homogeneous magnetic field along the z direction it would not generate a permanent circulation of the type shown in Figure 2. What is required in order to induce such an anapole is a magnetic field that would run along the spine or internal loop of a torus. Such a field is necessarily inhomogeneous and requires specially designed magnet geometries.[20] However, if the toroid is chiral the two types of motion will belong to the same Σ representation and can therefore be coupled. A homogeneous magnetic field along the z axis is then sufficient to induce an anapole moment: physically this means that in chiral tubes the current which goes around the central hole of the torus follows a spiral pattern, which includes a whirling of the $\Gamma(T_z)$-type. These effects have indeed been demonstrated by model calculations on small toroidal carbon cages.[21]

Chemistry has made steady progress towards the development of toroidal polyhedra, formed by a molecular network that can be mapped on the surface of a torus or doughnut. First Liu et al.[22] reported the observation of closed tubular structures in a batch of multiwalled nanotubes. Later on it was shown by Martel et al.[23] that single-walled carbon nanotubes could be bent by treatment with ultrasonic waves. The STM images of these structures show nice toroidal shapes, but the authors warn that these are very likely coils rather than tori. Very recently Sano et al.[24]

have managed to induce chemical bonds between the functionalised edges of a nanotube.

5. Complexes and Bundles

So far we have defined a polyhedral complex as a set of vertices with edge and face relationships. We now come to the next step, which is to define functions, which are centred at the vertex positions. As an example we may be interested in the elastic properties of clusters. In that case we define on each cluster atom, three Cartesian displacement coordinates and solve the equation of motion in this space of $3v$ displacements.

The special mathematical structure which is created in this way has the following ingredients: i) the set of vertex points or nodes of the complex, referred to as the base space B, ii) a unitary model space of functions, W, representing the object which will be associated with the individual vertices, in our example W contains the three Cartesian displacements, $W = (\Delta x, \Delta y, \Delta z)$, and $W_i = (\Delta x_i, \Delta y_i, \Delta z_i)$ then corresponds to the Cartesian displacements of vertex v^i, iii) the total function space containing all $3v$ displacements of the complex, $E = \{W_i\}_{i=1,v}$ and finally iv) the projection p which connects a given object to its node, $pW_i = v^i$. This link constitutes a fibre, and the total structure (E, B, W, p) is a fibre bundle.[25] With this structure our next task is to find out what happens to the topological invariants, which we have detected in the base space. Hence, what will be the functional forms they connect to?

Again this question can be solved by group-theoretical means. We first derive the symmetry representations of the functional space, and then insert in these expressions the symmetry relations of section 3.

We will illustrate this for the case of the displacement space. To obtain the answer we need to look at a fundamental result of the theory of induced representations.[7,26] It states that the representation of the $3v$ displacements of a cluster with v vertices or atoms is simply given by the direct product of the vertex representation, $\Gamma_\sigma(v)$, with the symmetry of the three translations, $\Gamma(T)$; Equation (20).

$$\Gamma_{x,y,z}(v) = \Gamma_\sigma(v) \times \Gamma(T) \tag{20}$$

This product representation is usually called the mechanical representation, while the vertex representation is obviously the positional representation. The connection in this case is obviously very simple, since it takes the form of a direct product.

We can now substitute the vertex term to yield Equation (21).

$$\Gamma_{x,y,z}(v) = [\Gamma_\parallel(e) - \Gamma_\odot(f)] \times \Gamma(T) + [\Gamma_0 + \Gamma_\epsilon] \times \Gamma(T) \tag{21}$$

The invariants in this equation are both multiplied by $\Gamma(T)$. These products can easily be evaluated, since multiplication with the totally symmetric representation, Γ_0, is a unit operation, while multiplication with the pseudo-scalar representation, Γ_ε, changes the parity and thus turns translations into rotations, see Equation (22).

$$\begin{aligned} \Gamma_0 \times \Gamma(T) &= \Gamma(T) \\ \Gamma_\epsilon \times \Gamma(T) &= \Gamma(R) \end{aligned} \tag{22}$$

Hence the forms in the displacement space, which correspond to the topological invariants of the positional space, are found to transform as the translations and rotations. The topological invariants of the complex thus connect to the collective motions that form the six external degrees of freedom of the cluster. In view of this special topological connection, these are indeed separate solutions of the displacement problem that cannot mix with the internal elastic modes.

In the next section we will show how the mechanical representation can further be resolved in the case of deltahedral clusters. In a further application we will also meet these special functional forms in the Fermi region of fullerene clusters.

6. Applications

Here we review two applications where functions are defined on a complex. One concerns atomic displacements, and the other atomic orbitals.

6.1 The Complete Force Field of Deltahedral Clusters

A deltahedral cluster is made up of triangles. The prototype is the closoborane series, $B_nH_n^{2-}$. Through the isolobal analogy several carbonyl transition-metal clusters have been synthesised with similar structures.

Deltahedral polyhedra are the dual forms of the trivalent polyhedra, discussed in section 4.1. The Euler relationship for trivalent cages, $3v = 2e$ [Equation (14)], can thus be converted into its dual form, which is valid for deltahedral cages; Equation (23).

$$3f = 2e \tag{23}$$

By combining this expression with Euler's theorem, we obtain a relationship between numbers of vertices and edges; Equation (24).

$$3v - 6 = e \tag{24}$$

One immediately recognises in this equation the number of internal degrees of freedom $3v - 6$ of a molecule with v atoms. This number is equal to the number of edges, e. The necessary and sufficient condition that the set of all stretch-

ings of edges would form a nonredundant set of vibrational coordinates is that not only the number but also the symmetries coincide. This equivalence of the vibrational and edge representation is indeed a fact for all deltahedra that can be mapped on the surface of a sphere. The proof is contained in the following fibre equation,[8] that is valid for deltahedra; Equation (25).

$$\Gamma_\sigma(v) \times \Gamma(T) - \Gamma(T) - \Gamma(R) = \Gamma_\sigma(e) \tag{25}$$

On the left the first term of dimension $3v$ is the representation of all Cartesian displacements of all atoms. From this we subtract the six external modes, comprising the translations and rotations. On the right $\Gamma_\sigma(e)$ is the symmetry representation of the set of edge centres. The stretching of an edge is σ-symmetric with respect to all symmetry elements going through the edge, and therefore is also covered by $\Gamma_\sigma(e)$. This expression is highly relevant for the force field of deltahedral clusters. It states that the symmetries of the displacements of the cluster atoms span the symmetries of the edge stretchings plus the six external degrees of freedom. Hence the edge stretchings exactly match the internal degrees of freedom. By putting a spring on every edge of a deltahedral cluster we construct a complete force field. The potential energy of this cluster can thus be written as given in Equation (26), where $\langle ij \rangle$ is the edge between atoms i and j and the summation runs over all edge pairs.

$$2V = \sum_{\langle ij \rangle \langle mn \rangle} k_{\langle ij \rangle \langle mn \rangle} \Delta r_{\langle ij \rangle} \Delta r_{\langle mn \rangle} \tag{26}$$

This equation is a typical example of a polyhedral relationship: a property of the vertices, in this case a displacement, is related to a property of a higher structural component, here the stretching of an edge. A mechanical proof of this property was already known to the famous French engineer and geometrician, Cauchy.[27] Boyle and Parker,[28] in their study of force fields in dodecaborane, noted the peculiar identity of the symmetries of the internal modes and the edge stretchings, but did not realise it was a general result for all deltahedra, which derives directly from the symmetry extension of Euler's theorem.

Table 4. Force constants for B_{12} in N/m

constant		value
k_1	$\langle ij \rangle \langle ij \rangle$	221.48
k_2	$\langle ij \rangle \langle im \rangle$	-33.12
k_3	$\langle ij \rangle \langle ik \rangle$	41.46
k_4	$\langle ij \rangle \langle km \rangle$	-29.57
k_5	$\langle ij \rangle \langle lm \rangle$	-17.36
k_6	$\langle ij \rangle \langle kl \rangle$	17.56
k_7	$\langle ij \rangle \langle kn \rangle$	0.88
k_8	$\langle ij \rangle \langle ln \rangle$	-3.95
k_9	$\langle ij \rangle \langle no \rangle$	8.06

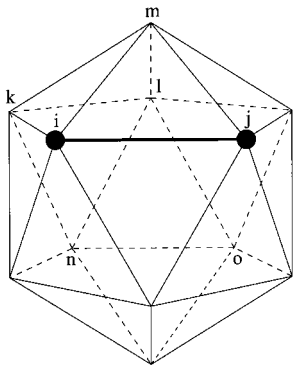

Figure 3. Vertex labelling for the boron skeleton in dodecaborane

In a recent study,[29] we have calculated the Hessian for $B_{12}H_{12}^{2-}$, using DFT techniques, and then derived the force constants. The results are listed in Table 4, following the bond labelling in Figure 3. It can be seen that the interactions between the bond stretchings decrease when the bonds are further apart, but quite remarkably, even bonds that do not have a common atom, still interact significantly. This confirms the delocalised nature of the bonding in these electron-deficient compounds.

6.2 The Frontier Orbitals of Fullerenes

In the innumerable fullerene family, Buckminsterfullerene, C_{60}, stands out in several ways. It is the smallest cage where all pentagons are isolated, and this contributes greatly to its stability, but in addition it is also a closed-shell molecule. In this respect it is the smallest member of the leapfrog class of closed-shell fullerenes.[30] A leapfrog fullerene, C_{3v}, is constructed from a smaller fullerene, C_v, by first capping all of its faces and then taking the dual of the resulting polyhedron. Since the smallest fullerene is the dodecahedron with twenty carbon atoms, the smallest leapfrog fullerene will indeed be C_{60}.[31]

The leapfrog construction (Figure 4) implies that the vertices in the parent will be transformed into hexagonal faces in the leapfrog. As a result all original faces will be surrounded by a ring of hexagons. This corresponds precisely to the "dilution" of the dodecahedron by hexagons to produce the familiar football shape.

The edges of the parent are also present in the leapfrog but are rotated by 90°. In C_{60} they correspond to the thirty edges separating the hexagons.

As a result the π-bonding in a leapfrog can be described by two extreme bonding schemes: either we put ethylenic bonds on all edges, that are derived from the edges of the parent cage, or we put aromatic sextets to all faces that are derived from the parent faces.

In Figure 5 these bonding extremes are connected in a Walsh-like correlation diagram, where we can move from the left to the right by gradually increasing the double-bond lengths and decreasing the single-bond lengths.[32]

On the left we have thirty isolated double bonds and thus thirty π-bonding orbitals and an equal number of π-anti-

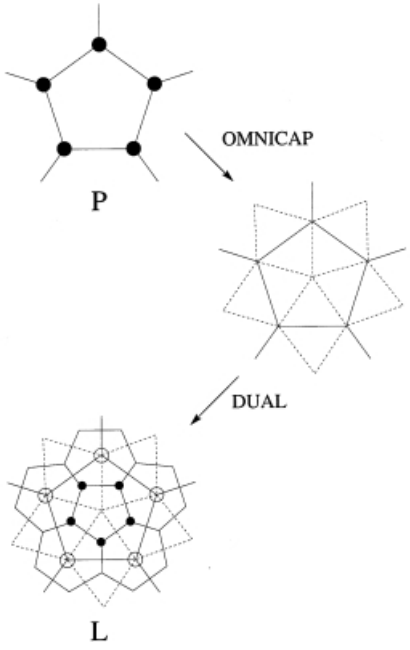

Figure 4. The leapfrog transformation; P is a piece of the parent, L is the leapfrog; vertices in P are hexagon centres in L; faces in P remain faces in L

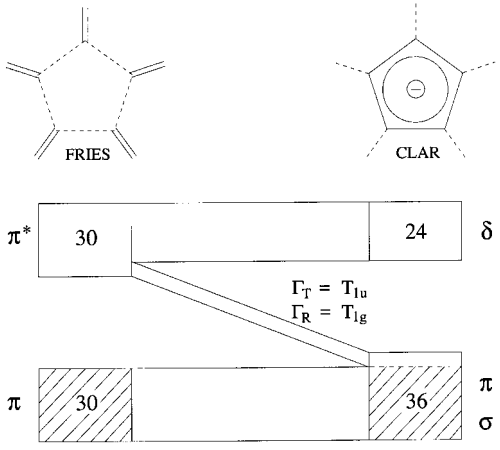

Figure 5. Walsh diagram for C_{60} with correlation between two bonding extremes: a "Fries" structure on the left with localised double bonds between pentagons, and a "Clar" structure on the right with aromatic sextets on the pentagon

bonding orbitals. On the right we recognise the bonding orbitals of twelve isolated pentagons, with the bonding σ and π shells that form the aromatic sextet, and antibonding δ-type orbitals. When we move away from the bonding extremes the localised levels broaden and become the molecular orbitals of C_{60}. Quite remarkably, the *symmetries* of all thirty bonding combinations on the left are present in the thirty-six bonding combinations on the right. The six remaining combinations will correlate with the π* orbitals on the left, and cross the nonbonding line almost halfway between the two extremes. As a result C_{60} has a closed shell of thirty bonding orbitals, followed by a set of low-lying almost nonbonding orbitals. These transform in icosahedral symmetry as T_{1u} and T_{1g} representations, which happen to be the representations of translation and rotation.

This pattern is characteristic for all leapfrog fullerenes. There is always a set of six low-lying frontier orbitals with the $\Gamma(T) + \Gamma(R)$ symmetry. For a general leapfrog fullerene the number of bonding orbitals on the left will be equal to the number of edges, *e*, in the parent. Similarly, the number of bonding orbitals on the right will be equal to three times the number of faces, 3*f*, in the parent. These numbers indeed differ by six, see Equation (27), which follows from Euler's rule, for trivalent cages.

$$e = 3f - 6 \tag{27}$$

As in the previous example, for the correlation in the Walsh diagram to hold, more is required than a simple dimensional agreement. The symmetries of the bonding orbitals on the left should match the symmetries on the right. This is indeed the case according to the following fibre rule for trivalent cages, which is of course the dual of the fibre rule for deltahedra in Equation (25), see Equation (28).

$$\Gamma_\sigma(e) = \Gamma_\sigma(f) \times \Gamma(T) - \Gamma(T) - \Gamma(R) \tag{28}$$

The $\Gamma_\sigma(e)$ term in this equation precisely corresponds to the symmetries of ethylenic bonding orbitals on the edges of the parent, since these are symmetric combinations of the p_z orbitals at either end of the edge. The left-hand side of the expression thus describes the symmetries of the bonding combinations on the left of the Walsh diagram. Similarly, the term $\Gamma_\sigma(f) \times \Gamma(T)$ spans the symmetries of the aromatic sextets on the right of the diagram: each aromatic sextet comprises three orbitals which transform as σ, π_x, and π_y with respect to the centre of the pentagon: i.e. a set which transforms as the three Cartesian components. The direct product $\Gamma_\sigma(f) \times \Gamma(T)$ then generates the bonding orbitals on all twelve pentagons. The group-theoretical results then state that for any fullerene which is a leapfrog, matching of the two bonding extremes will provide a closed-shell structure, with a set of low-lying orbitals transforming as $\Gamma(T) + \Gamma(R)$.

These special frontier orbitals are once again defined as the fibre, which connects to the topological invariances of the polyhedral complex.

A similar analysis can also be extended to other trivalent cages containing triangular or quadrilateral defects. It has also been performed for the graphene sheet.[12] In this case the topologically relevant orbitals are identified as the four semi-occupied nonbonding orbitals in the K-point of the honeycomb lattice.

Conclusion

In many respects molecules are graph-like objects. The Hückel model is essentially based on the molecular graph. Probably in the whole of quantum chemistry, there isn't a

single theory that can compete with this model in terms of minimal effort for maximum relevance.

In this review we point to the existence of equally general molecular relationships, which go beyond the vertex-edge picture, and imply face structures. Especially in the area of clusters and network molecules this leads to useful new insights, both for the description of electronic and elastic properties. In the polyhedral complex steric aspects of molecular structure are taken into account. Note that the elements of a complex are not spatial coordinates, but relationships between atomic nodes.

Further theoretical efforts are certainly needed to expand the theoretical framework. The fibre bundles that we have considered in section 6 are indeed trivial examples, where the connection is a straightforward product. More intricate problems are offered by the description of tunnelling between Jahn−Teller minima on a surface. These await further analysis.

We finally hope the present microreview will invite chemists to acquire a practical understanding of topological concepts. Our main ally in applying these concepts to molecular properties clearly is group theory. Group theory and topology are not rival mathematical disciplines but go admirably together, reinforcing each others results.

Acknowledgments

Financial support from the Flemish Government (Concerted Action Scheme) and the Fund for Scientific research − Flanders (Belgium) is gratefully acknowledged. A. C. is greatly indebted to Patrick Fowler (Exeter) and Marek Szopa (Katowice) for extensive collaborations on the topic of this review during the past ten years.

[1] A. T. Balaban, *Chemical Applications of Graph Theory*, Academic Press, London, **1976**.
[2] A. R. Leach, *Molecular Modelling: Principles and Applications*, Longman, Harlow, **1996**.
[3] P. J. Giblin, *Graphs, Surfaces and Homology*, Chapman and Hall, London, **1977**.
[4] F. A. Cotton, *Chemical Applications of Group Theory*, 3rd ed., Wiley, New York, **1990**.
[5] P. J. Federico, *Descartes on Polyhedra*, Springer, New York, **1982**. A collection of proofs of the Euler theorem is assembled on web page http://www.ics.uci.edu/~eppstein/junkyard/euler
[6] For a thorough mathematical treatise on homologies, consult: P. J. Hilton, S. Wylie, *Homology Theory*, Cambridge University Press, Cambridge, **1960**.
[7] S. L. Altmann, *Induced Representations in Crystals and Molecules*, Academic Press, London, **1971**.
[8] A. Ceulemans, P. W. Fowler, *Nature (London)* **1991**, *353*, 52−54.
[9] A. Ceulemans, M. Szopa, P. W. Fowler, *Europhys. Lett.* **1996**, *36*, 645−649.
[10] P. W. Fowler, A. Rassat, A. Ceulemans, *J. Chem. Soc., Faraday Trans.* **1996**, *92*, 4877−4884.
[11] A. Ceulemans, P. W. Fowler, *J. Chem. Soc., Faraday Trans.* **1995**, *91*, 3089−3093.
[12] A. Ceulemans, L. F. Chibotaru, P. W. Fowler, M. Szopa, *J. Chem. Phys.* **1999**, *110*, 6916−6926.
[13] A. Ceulemans, R. B. King, S. A. Bovin, K. M. Rogers, A. Troisi, P. W. Fowler, *J. Math. Chem.* **1999**, *26*, 101−123.
[14] E. D. Jemmis, M. M. Balakrishnarajan, P. D. Pancharatna, *J. Am. Chem. Soc.* **2001**, *123*, 4313−4323.
[15] R. L. Johnston, *Struct. Bonding (Berlin, Ger.)* **1997**, *87*, 1−34.
[16] R. Hoffmann, *Angew. Chem. Int. Ed. Engl.* **1982**, *21*, 711−724.
[17] R. L. Johnston, D. M. P. Mingos, *J. Organomet. Chem.* **1985**, *280*, 407−418.
[18] D. M. P. Mingos, D. J. Wales, *Introduction to Cluster Chemistry*, Prentice Hall, Englewood Cliffs, New York, **1990**.
[19] B. Y. Zel'dovich, *Zh. Eksp. Teor. Fiz.* **1957**, *33*, 1531.
[20] D. Loss, P. Goldbart, A. V. Balatsky, *Phys. Rev. Lett.* **1990**, *65*, 1655−1658.
[21] A. Ceulemans, L. F. Chibotaru, P. W. Fowler, *Phys. Rev. Lett.* **1998**, *80*, 1861−1864.
[22] J. Liu, H. J. Dai, J. H. Hafner, D. T. Colbert, R. E. Smalley, S. J. Tans, C. Dekker, *Nature (London)* **1997**, *385*, 780−781.
[23] R. Martel, H. R. Shea, P. Avouris, *J. Phys. Chem. B* **1999**, *103*, 7551−7556.
[24] M. Sano, A. Kamino, J. Okamuri, S. Shinkay, *Science* **2001**, *293*, 1299−1301.
[25] J. Biel, R. Chatterjee, T. Lulek, *J. Chem. Phys.* **1987**, *86*, 4531−4540.
[26] A. Ceulemans, *Mol. Phys.* **1985**, *54*, 161−181.
[27] A. L. Cauchy, *J. Ec. Imp. Polytech. (Paris)* **1813**, *19*, 87−98.
[28] L. L. Boyle, Y. M. Parker, *Mol. Phys.* **1980**, *39*, 95−109.
[29] A. Ceulemans, B. C. Titeca, L. F. Chibotaru, I. Vos, P. W. Fowler, *J. Phys. Chem. A* **2001**, *105*, 8284−8295.
[30] P. W. Fowler, J. I. Steer, *J. Chem. Soc., Chem. Commun.* **1987**, 1403−1405.
[31] D. E. Manolopoulos, P. W. Fowler, *An Atlas of Fullerenes*, Clarendon Press, Oxford, **1995**.
[32] P. W. Fowler, A. Ceulemans, *J. Phys. Chem.* **1995**, *99*, 508−510.

Received October 16, 2001
[I01411]